CH-GFZ-TR-2501

Overhauser Magnetometer

Performance Test Report

	Name	Date and Signature
Prepared by:	H. Lühr, R. Bock, M. Rother (GFZ)	*H. Lühr, R. Bock*
Checked by:	J.-M. Leger (LETI)	
Project Management:	Prof. Dr. Ch. Reigber (GFZ)	*Ch. Reigber 7.7.99*

Document Change Record

Issue	Date	Page	Description of Change
1.0	06.04.98	all	First Issue
1.1	01.02.99	3	Abstract included
		5	Chapter 2 'Relevant Documents' included
		6	Time interval for noise spectra
		11	Updated values
		12	Updated tables OVM response to a 1-Hz synchronised step function
		14-16	Heading error determination
		16-17	Temperature dependence

ABSTRACT

This report comprises the results of the performance test conducted with the Overhauser Magnetormeter (OVM) at the LETI magnetic facility in Herbeys/France. Of special interest are the critical parameters determining the quality of the instrument and their behaviour over the nominal operation (full performance) temperature range (-20...+40 °C). Subsequently the major results are listed (requirements in parenthesis).

- The noise level within the dynamic range was found to be 70 pT_{rms} @ 18000 nT and 20 pT_{rms} @ 40000 nT and above (resolution: 100 pT).

- The dynamic behaviour reflects perfectly the specified filter characteristics with a -3dB cut off frequency at 0.28 Hz.

- Deviations from an omnidirectional sensitivity were found to be <230 pT.

- Temperature dependent field changes over the full performance range are <150 pT (absolute accuracy <0.5 nT).

This test showed the outstanding performance of the CHAMP OVM surpassing the requirements in all points.

LIST OF CONTENTS

1 INTRODUCTION

The Overhauser Magnetometer (OVM) on CHAMP is intended to serve as a magnetic standard during the 5 years mission. The OVM measures the magnetic field magnitude which will be used to calibrate the vector measurements of the Fluxgate Magnetometers (FGM). The main purpose of the test was to verify the absolute accuracy of the instrument under all kinds of environmental conditions and demonstrate the required performance.

The Performance Test was carried out during the week February 9 to 13, 1998, at the magnetic test facility of the instrument provider LETI. The test site is located on the fringes of the small mountain village Herbeys some 10 km to the south-east of Grenoble. The exact coordinates of the place are: 45.129°N and 5.806°E, height above sea level is about 500 m.

The magnetic field magnitude observed during the test ranged around 46400 nT. From the magnetic field model IGRF95 we derived angles for the declination and inclination of -0.8° and 61°, respectively. During the first day of the test the magnetic activity was rather low. On the second, however, a major magnetic storm commenced and lasted into the third. Since all measurements were made in parallel with closely spaced reference sensors, the magnetic activity did not influence the quality of the results.

The results obtained during this test contain important parameters characterising the instrument. A part of them will directly enter the data processing software. Of special interest are those measurements which characterise the limits of the OVM. Unfortunately the test had to be terminated on the last day due to technical problems during the thermal run of the electronics box. The instrument failed to go in lock at low temperature. The performance test will be repeated at a later time.

A good part of the tests performed in February 1998 were repeated in the May/June time frame. In this new issue later results on the step response, the heading error and the temperature dependence of the instrument have been taken into account.

2 RELEVANT DOCUMENTS

We will refer to the following documents in this report

[RD 01]   CH-GFZ-SP-0025, issue 1.2
Overhauser Magnetometer Specification

[RD 02]   DSYS/CSME/200798/A087
CHAMP Overhauser Magnetometer Functional Test

[RD 03]   IAGA News 30, pp.78, 1991

3 SENSOR NOISE FIGURES

A quantity limiting the resolution of an instrument is its noise level. For the determination of the instrument noise the Overhauser sensor was exposed to the ambient magnetic field. Two nearby sensors termed Ref (1) and Ref (2) were used to monitor the natural variations. In order to test the dependence of the instrument noise on the field intensity the OVM sensor was placed in a coil system which allowed to apply field strengths up to 80 µT.

The obtained results are illustrated in the Figures 3-1 to 3-3. First we give an overview of the performance of the test setup. The upper left panel of Figure 3-1 shows ambient field variations during one test period. Field variations were fairly large due to the above mentioned magnetic storm in progress. To overcome this problem we only employed differential measurements between two closely spaced sensors. The quality of this method is shown in the upper right

panel of Figure 3-1. Here the differences between the readings of the two sensors Ref (1) and Ref (2) is plotted. No signature of the original time series is left only uncorrelated noise with peak-to-peak amplitudes of ±20 pT. We regard this as a prove of the differential method and the quality of the reference sensors.

For the evaluation of the noise measurements we always subtracted Ref (1) from the OVM readings. As can be seen from the lower left panel in Figure 3-1, the noise amplitude of the OVM reaches peak values of about ±50 pT. During the mission it is foreseen to perform some smoothing of the data in the post processing. Here we applied a simple digital filter of the form

$$Y = \frac{1}{8}X_1 + \frac{3}{8}X_2 + \frac{3}{8}X_3 + \frac{1}{8}X_4 \tag{1}$$

where X_n are successive readings. This filter reduces the noise amplitude by about a factor of 2 (see lower right panel).

A presentation of all the above mentioned signals in the frequency domain is given in Figure 3-2. The two top panels show the spectra of the ambient variations recorded by the reference sensors. They are almost identical to the spectrum obtained by the OVM which is shown in the middle right panel.

The differences between the two reference sensors (panel at middle left) exhibit a spectral peak around 0.5 Hz at a very low level of 1 pT demonstrating the reliability of the reference measurements. The spectrum of the OVM noise (bottom left) derived from the difference between OVM and Ref (1) measurements peaks around 0.4 Hz with an amplitude of 3 pT. When applying the above described filter primarily the high frequency part beyond the peak will be attenuated (bottom right).

So far we have discussed in some detail the results of the noise measurements at ambient field strength. For the characterisation of the OVM it is, however, important to know the noise figures over the whole specified measurement range. Noise spectra determined over a period of 500 s for various field strengths are given in Figure 3-3. The headlines of the diagrams contain the field strength in µT. At 18 µT, the lower limit of the measurement range, the noise level is significantly enhanced. With increasing field strength the noise spectra decrease until they reach a constant level for field strengths beyond 30 µT. In this range we find the spectral peak around 0.4 Hz at an amplitude of 3 pT. Depending on the signal spectrum during the mission this peak value could be lowered by post filtering.

In summary, we may state that the noise level of the OVM is sufficiently low to allow for the specified resolution of 100 pT over the whole measurement range.
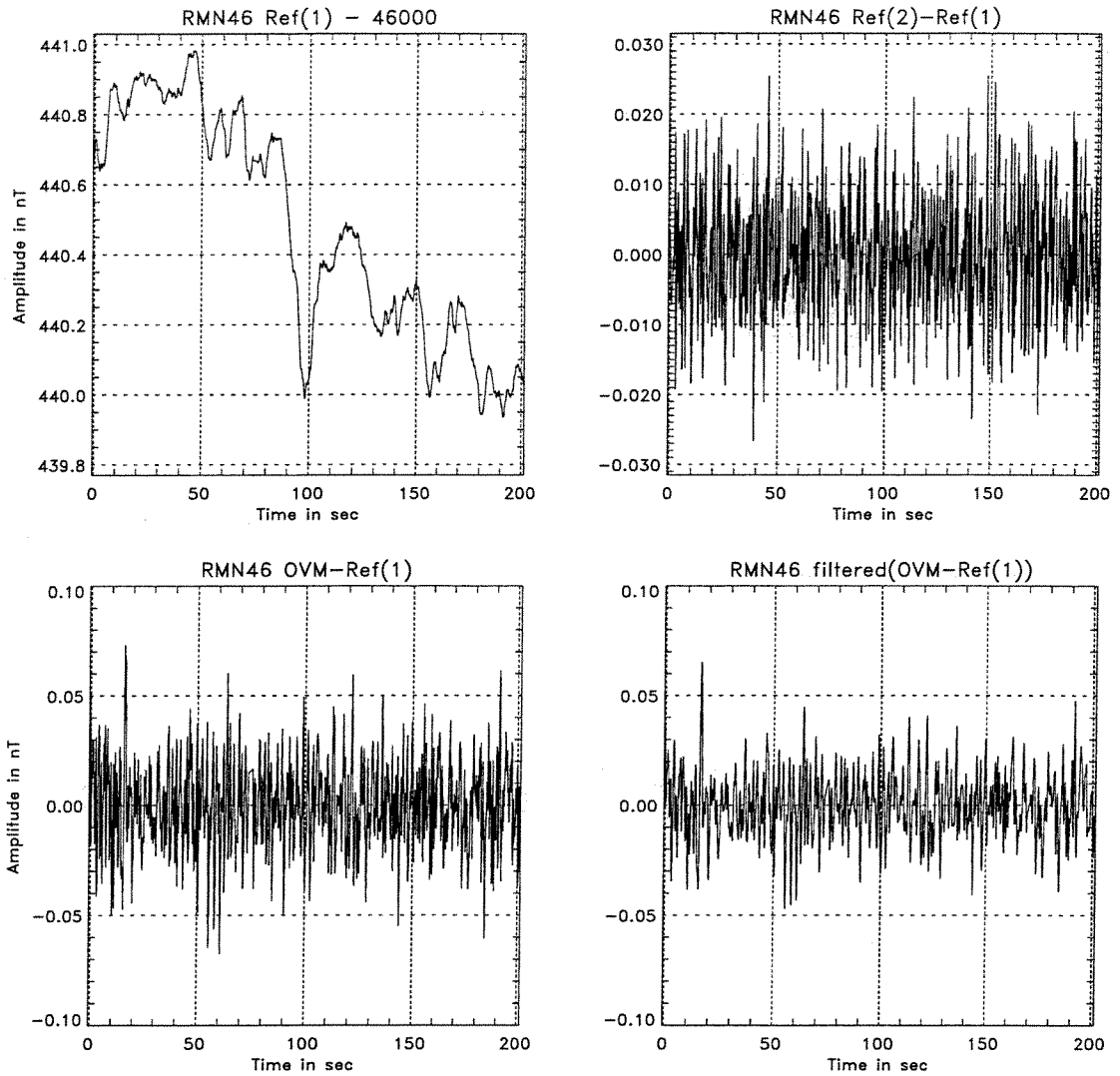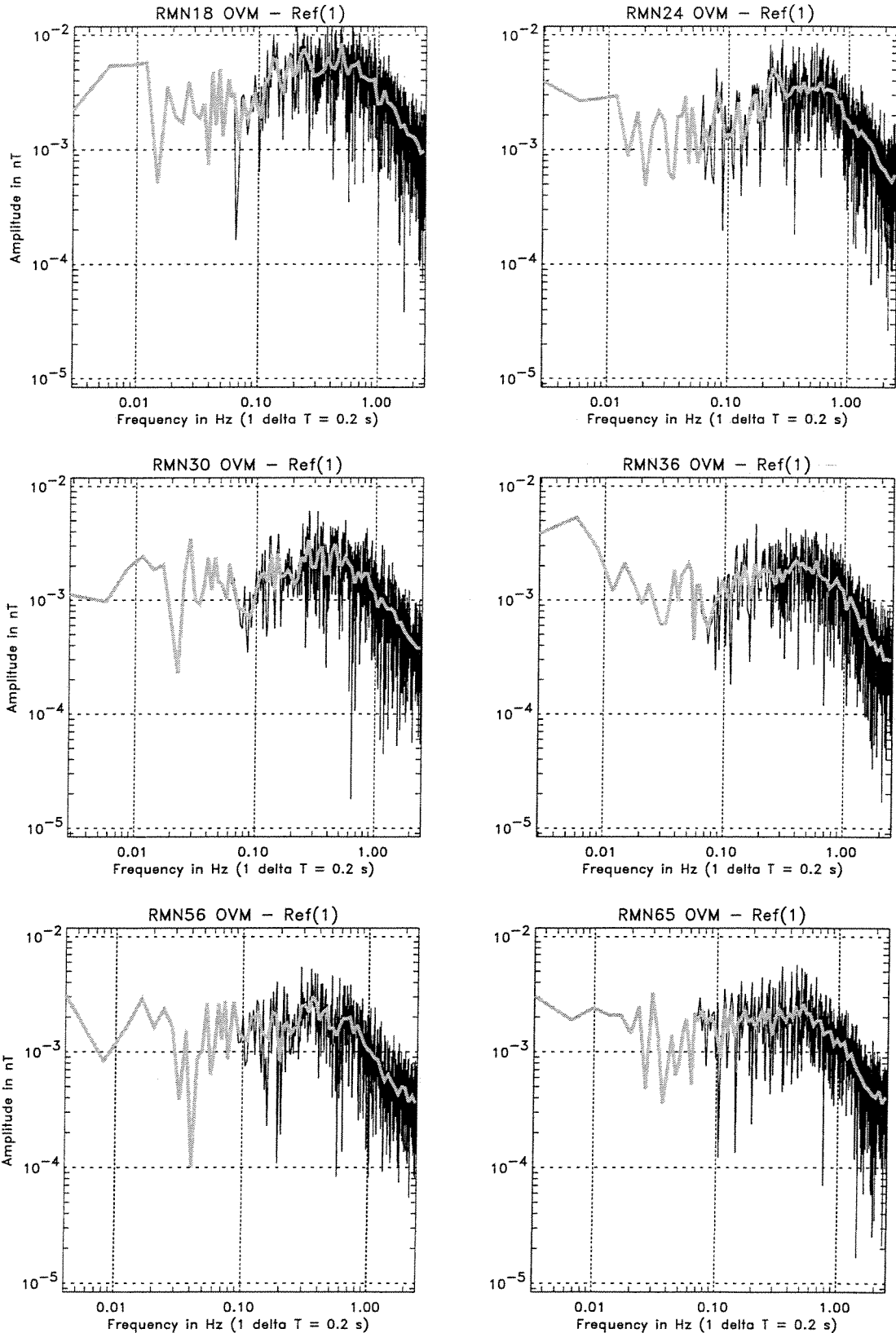
-/plt/blatt3.eps Wed Apr 22 13:25:31 1998

Figure 3-1   Magnetic signals obtained at ambient field strength
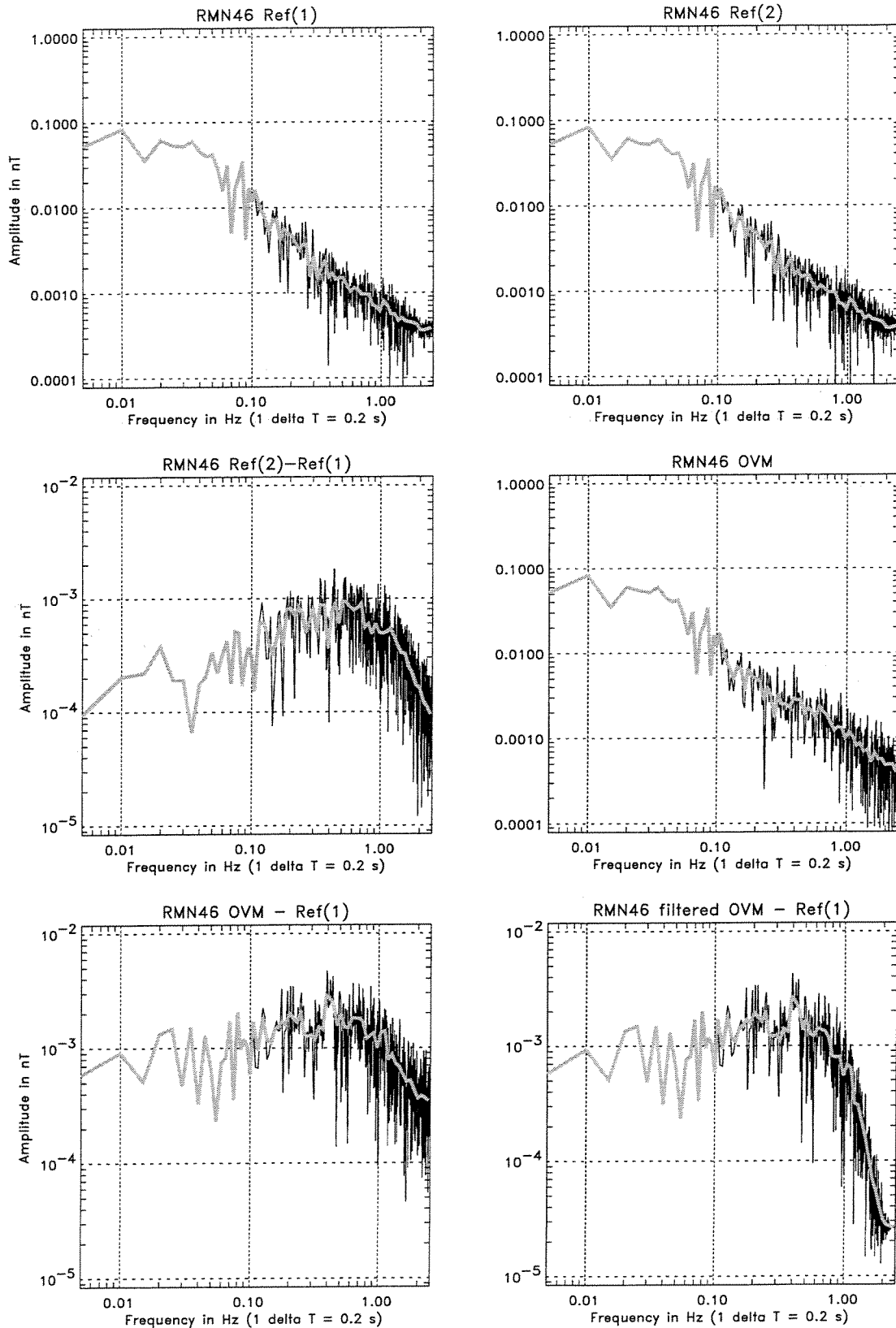
-/plt/blatt1.eps Wed Apr 22 13:25:00 1998

Figure 3-2   Signal and noise spectra obtained at ambient field strength

-/plt/blatt2.eps Wed Apr 22 13:25:01 1998

Figure 3-3   OVM noise spectra at various field strengths

4 FIELD LOCKING PROCEDURE

For the precise measurement of the proton Larmor frequency the signal of the Overhauser sensor is passed through a phase lock loop circuit. A critical situation for this circuit is the initial period of frequency acquisition. After switch-on the instrument starts the search at the high-field end (65 µT) and sweeps down to the lower end (18 µT). In case of an unsuccessful search it jumps to a fixed frequency equivalent to 50 µT. This field value was chosen, since 50 µT has the highest occurrence probability over the CHAMP orbit.

For the test of the locking procedure a magnetic field was applied to the sensor which was rising at a rate of 100 nT/s. During the mission maximum change rates will be less than 30 nT/s. At the same time the internal frequency search scans downward from the high-field end. At the cross-over of both frequencies the instrument should lock and track the field changes. We have started the external rising fields from various level and initiated at the same time the frequency search. The table below shows how long it took until locking was achieved.

Start value	Time till lock
65 µT	5 sec
60 µT	15 sec
55 µT	25 sec
50 µT	33 sec
45 µT	40 sec
40 µT	50 sec
35 µT	65 sec
30 µT	85 sec
25 µT	120 sec
20 µT	150 sec
18 µT	200 sec

Field locking was obtained in all cases after the expected time. In case of a provoked unsuccessful search (field too low) the seed field value jumped to 49920 nT and stayed there as expected.

For testing the signal margin during the locking procedure white noise with an amplitude density of $10 \, pT/\sqrt{Hz}$ was added to the sensor on top of the ambient field strength of 46 µT. The instrument still managed to lock but for any higher noise level it did not.

Finally we tried to find the lowest field strength the instrument is capable to track. For that purpose the OVM was first brought into lock and then the field applied to the sensor slowly reduced. At 9 µT the OVM lost track of the field. This has to be compared to the instrument specification which requires a lower limit of the measurement range of at least 18 µT.

5 FREQUENCY RESPONSE OF OVM

The Larmor frequency of the protons, which is a measure for the field strength, is measured very frequently. The readings are filtered digitally and samples are output every second. The filter used is of recurrent type (IIR).

$$y_n = \frac{q-1}{q} y_{n-1} + \frac{1}{q} x_n \tag{2}$$

where x_n is the current reading of the frequency meter and $q = 1025$ in the case of CHAMP. This filter is applied three times to the data.

Recurrent filters can be described more handy in the frequency domain. The amplification factor v amounts to

$$v = \frac{1}{1 + i\omega Q} \tag{3}$$

where ω is the angular frequency and Q is a characteristic constant of the filter, replacing RC of hardware filters.

$$Q = \frac{q}{p} \tag{4}$$

where $p = 3571.5$ is the rate at which the frequency meter is sampled in the case of CHAMP. We thus obtain $Q = 0.287$.

Since the filter cell is used three times in series, we obtain for the amplitude factor

$$v^2 = \frac{1}{\left(1 + (\omega Q)^2\right)^3} \tag{5}$$

and for the phase

$$\phi = 3 \arctan(\omega Q) \tag{6}$$

The resulting -3 dB frequency is $f_c = 0.283$ Hz.

Recurrent filters have a phase delay which is in general depending on the frequency. For all practical purposes we can, however, consider the resulting group delay $\tau = 0.861$ sec as constant.

During the performance test sinusoidal fields with an amplitude of 73 nT have been added to the ambient field of 46 442 nT. Both measured and computed amplification factors are listed below.

Frequency	v (measured)	v (computed)
5 mHz	1.0	0.9999
10 mHz	1.0	0.9995
20 mHz	0.9994	0.9981
50 mHz	0.9877	0.9879
100 mHz	0.9521	0.9531
200 mHz	0.8329	0.8324
450 mHz	0.4712	0.4682
1.01 Hz	0.1130	0.1115
2.05 Hz	0.0181	0.0178

The excellent agreement between the predicted and observed attenuation demonstrates that our analytical description of the filter is correct and that the derived characteristic parameters like cut-off frequency and group delay time are applicable.

In another test the response of the instrument to step-like field changes was investigated. If the instrument would follow a field change instantaneously, only the step response of the filter should modify the data. For the step response of the above filter type we can give an analytical description

$$b(t) = b_S - b_S \, e^{-T} \left(1 + T + \tfrac{1}{2} T^2 \right) \tag{7}$$

where b_S is the size of the field step and $T = t/Q$. For a normalised step we compute the following response curve

t, sec	b(t)
0	0.0
1	0.6762
2	0.9697
3	0.9981
4	0.9999

Within 4 sec after the change the new level is acquired.

During the test we have applied field steps of various heights, starting with 10 nT and ending at 10 000 nT. The instrument could track the changes safely up to 5 000 nT. In order to check the dynamic performance of the instrument a fit of the response function to the readings both for upward and downward cases was performed. The residuals are in general around 0.1 nT for step sizes below 1 000 nT (cf. chapter 10 Appendix A), for larger changes they grow proportionally with the amplitude reaching some 5 nT at 5 000 nT steps.

In a later test the response of the OVM to a step function synchronised to the 1-Hz synchronisation pulse was investigated. The applied square wave signal was high for 16 sec and then low for another 16 sec allowing for a sufficient settling time of the filter. The level change took place exactly in the middle between adjacent synchronisation pulses. We have fitted the expected step response to the actually measured signal shape using the start time as a free fit parameter. Print outs of the results can be found in Appendix B. The obtained start times coincide precisely with the time of level switch for step sizes of 20 nT. They are slightly

delayed by 1 and 2 ms for 50 nT and 100 nT steps, respectively. The residuals are again in the range of 0.1 nT and reflect the variability of the ambient field. From the results obtained we can conclude that no further time delays others then those caused by the filter have to be taken into account.

This result shows that for all practical purposes we can assume the instrument is tracking field changes according to its response characteristic. This is of special interest for the elimination of the magnetic field disturbances caused by the magnetic torquer coils.

6 DETERMINATION OF FIELD / FREQUENCY RELATION

The advantage of proton precession magnetometers is that they make use of the fact that the Lamor frequency of the protons is directly related to the ambient field by an atomic constant. The linking number is called the *gyro magnetic ratio*. To make sure that the required frequency measurements do not suffer from drifts during the mission the local oscillator is continuously checked against GPS time.

For the check of the implemented *gyro magnetic ratio* (γ_P) we excited the sensor from outside at a frequency of 1.9067694 kHz. This resulted in a field reading of 44 785.13 nT. At the same time the number of counts of the local oscillator between two pulses of the PPS-signal (pulse per second) was 3 656 731 while the period between subsequent PPSs was 0.99985993 sec. The nominal frequency of the local oscillator should be 3 657 250 Hz. From these numbers we can compute the *gyro magnetic ratio* used in this instrument

$$\gamma_{P,OVM} = \frac{44785.13}{1906.7694} \frac{3656731}{0.99985993} \frac{1}{3657250} = 23.487396 \frac{nT}{Hz} \tag{8}$$

The actually implemented value is 23.48741 thus the obtained difference of $6 \cdot 10^{-7}$ is of no significance. The recommended value for geophysical measurements is

$$\gamma_{P,IAGA} = 23.4872038 \frac{nT}{Hz} \qquad \text{[RD 03]}$$

The actual readings obtained during the mission have to be re-scaled by using the housekeeping reading HK_{Quartz} in the following way:

$$B = B_{OVM} \frac{\gamma_{P,IAGA}}{\gamma_{P,OVM}} \frac{HK_{Quartz}}{3657250} \tag{9}$$

7 DETERMINATION OF SENSOR HEADING ERROR

An important feature when assessing the absolute accuracy of proton magnetometers like the OVM is to know the heading error which is caused by magnetised material in the vicinity of the sensor. In case the error is caused by a field source fixed to the sensor the readings of the field modules will be modified in the following way

$$B^2 = (X + X_0)^2 + (Y + Y_0)^2 + (Z + Z_0)^2 \tag{10}$$

where X,Y and Z are the field components of the ambient field in a sensor fixed frame and X_0, Y_0 and Z_0 are the components of the heading error.

To determine the heading error the OVM sensor was oriented in many different directions with respect to the ambient field. Simultaneously with the OVM readings measurements were taken by two reference scalar magnetometers located 1 m and 4 m apart. The differences b between OVM readings and the reference magnetometers can be written as

$$b = \sqrt{(X + X_0)^2 + (Y + Y_0)^2 + (Z + Z_0)^2} - B_{ref} \tag{11}$$

Using the reasonable assumption that the heading error is much smaller than the ambient field we may linearise the equation and get

$$bB_{ref} = XX_0 + YY_0 + ZZ_0 \tag{12}$$

When employing measurements from various sensor orientations we can solve the system of linear equations for the components X_0, Y_0 and Z_0.

During the Performance Test a set of measurements was obtained while rotating the sensor about its x axis, later it was rotated about the y axis. For the definition of the body-fixed coordinates x, y, z see Figure 7-1. The field components X, Y, Z in equations (10) through (12) have to be computed from the local geomagnetic elements as given in Section 1. For the first rotation we get

$$X = -B\sin I \quad , \quad Y = B\cos I \sin\phi \quad , \quad Z = -B\cos I \cos\phi \tag{13}$$

where I is the inclination angle and ϕ is the angle of rotation. Readings were taken at intervals of 45°. For the other rotation the field components can be computed as

$$X = -B\sin(I - \phi) \quad , \quad Y = 0 \quad , \quad Z = -B\cos(I - \phi) \tag{14}$$

In this case readings were taken only in steps of 90° governed by the requirement of a safe positioning of the sensor.

By combining both sets of measurements and correcting for constant field gradients between the OVM and the reference sensors we solved equation (12) for the heading error. The obtained result is

$$X_0 = 210\,pT \quad , \quad Y_0 = 130\,pT \quad , \quad Z_0 = 290\,pT$$

In a later test the determination of the heading error was repeated with an improved test setup [RD 02]. With the help of the turntable the sensor was rotated about two perpendicular axes and the difference between the OVM readings and a reference sensor recorded. In the first case the sensor was rotated about the x axis while the rotation plane contained the local magnetic field and the east/west direction. For the phase angles $\varphi = 0°$ and $\varphi = 90°$ z pointed along B and towards east, respectively. During the second run the sensor was rotated about the y axis which pointed towards west. For the phase angles $\varphi = 0°$ and $\varphi = 90°$ z pointed toward north and upward, respectively. Readings were taken every 30°. Results are given in Appendix C.

The field components X, Y, Z needed for solving Eq (12) can be computed for the two cases

$$X = 0 \quad , \quad Y = B\sin\phi \quad , \quad Z = B\cos\phi \tag{15}$$

$$X = -B\sin(I + \phi) \quad , \qquad Y = 0 \quad , \qquad Z = B\cos(I + \phi) \qquad (16)$$

By combining the two sets of measurements the heading error can be determined when solving Eq (12) for X_0, Y_0, Z_0. From the improved setup we obtain

$$X_0 = -178\,pT \quad , \qquad Y_0 = -35\,pT \quad , \qquad Z_0 = -138\,pT$$

Surprisingly all three components exhibit an opposite sign. Whereas their obtained magnitudes are of the same order.

In order to check the consistency of the latter results we have interpreted the two rotations individually by computing their Fourier transforms. The relevant coefficients are for the first rotation:

$$a_1 = -144.2\,pT \quad , \quad b_1 = 35.4\,pT \quad , \quad a_2 = 5.7\,pT \quad , \quad b_2 = -29.7\,pT$$

and the second rotation:

$$a_1 = 105.5\,pT \quad , \quad b_1 = 195.4\,pT \quad , \quad a_2 = -99.3\,pT \quad , \quad b_2 = 101.8\,pT$$

all higher terms can be attributed to quantisation noise.

The interpretation of the first rotation is according to Eq (15) straight forward ($Z_0 = a_1$, $Y_0 = -b_1$). We obtain:

$$Y_0 = -35.4\,pT \quad , \qquad Z_0 = -144.2\,pT$$

For the interpretation of the second run we have to rotate according to Eq (16) the coefficients by (-I) about the y axis. We obtain

$$X_0 = -187.0\,pT \quad , \qquad Z_0 = -119.6\,pT \qquad (I = 61°)$$

$$X_0 = -178.2\,pT \quad , \qquad Z_0 = -132.4\,pT \qquad (I = 65°)$$

If we allow for a somewhat elevated inclination, we can reproduce the above obtained numbers.

This small but significant bias could be corrected for during the data evaluation using the equation

$$B = B_{OVM} - \frac{XX_0 + YY_0 + ZZ_0}{B_{OVM}} \qquad (17)$$

where the field components X, Y and Z should be taken from the appropriate Fluxgate readings.

From the second run it is obvious that the second harmonic signal reaches an amplitude almost comparable with the first harmonic. While the first harmonic is caused by remanent magnetic parts on the sensor, the second harmonic may be attributed to the effect of soft magnetic material. The so-called static induced field depends on the magnitude of the ambient field. This effect is limited more or less to the x-z plane. When the ambient field is parallel to a line which connects the centre of the preamplifier with the centre of the sensor then we observe as expected an enhancement of the reading. In case of a field perpendicular to this line the output values are reduced. This effect can be corrected in the following way

$$B = B_{OVM} - \frac{0.14\left(X^2 - Z^2\right) + 1.5\,XZ}{B_{OVM} \cdot 10^6} \tag{18}$$
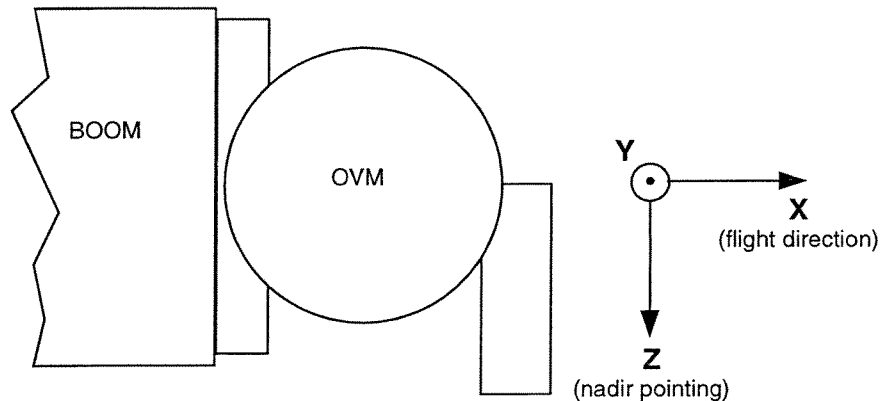

Figure 7-1   Body-fixed coordinate system of the OVM sensor

8 MAGNETIC MOMENT OF THE DPU

In a rather similar fashion as for the heading error the magnetic moment of the DPU was determined by twisting and turning the box 1 m apart from a reference sensor. It turned out that it exhibits both remanent and soft magnetic features.

Remanent field: 0.4 nT at 1 m in 2nd Gaussian orientation.

This results in a magnetic moment of m = 4 mA m² (allocation for the OVM-DPU: m = 20 mA m²).

Soft magnetic field: the ambient field is reduced by 0.5 nT at 1 m distance.

The effect of remanent and soft magnetisation will be corrected for on spacecraft level.

9 TEMPERATURE DEPENDENCE OF THE INSTRUMENT

As stated above the OVM is intended to act as a magnetic field standard. Temperature changes should thus not alter the readings. The purpose of this part of the test is twofold, to demonstrate the stability of the measurements over the specified temperature range and to determine the temperature dependent instrument parameters. The first part of the test which includes temperature cycling of the electronics box and the sensor while doing high performance measurements could not be complete because of problems with field locking at low temperatures.

During the time frame May, June 1998 several tests concerning the temperature dependence of the instrument were performed. Details of the results are given in [RD 02]. Both the DPU and the sensor were exposed individually to varying temperatures between -30° and 40°C.

In case of the DPU the magnetic field readings varied only by 25 pT over the whole range of 70K. A somewhat stronger dependence is observed when thermocycling the sensor. The readings go down by about 250 pT, roughly proportional with the temperature, when the sensor is cooled down from 40° to -30°C. The major part of this effect is probably due to a temperature gradient across the sensor, which is hard to avoid in a small thermal chamber.

As part of the telemetry 9 Housekeeping (HK) values are transmitted characterising the health of the instrument. Monitoring them over a range of temperatures allows to determine the temperature dependence of individual parameters.

The three HK channels monitoring the supply voltages 10 V, -10 V and 15 V showed no variations with temperature. The same is true for the 60 MHz signal. Both the power (HF-Level) and the amplitude (HF-Adaption) of the sensor excitation signal are rather independent of the ambient temperature.

A real variation with temperature is observed for the frequency of the quartz oscillator. As can be seen in Figure 9-1 it changes quite linearly wrt. temperature (-1.27 Hz/K). Since this oscillator provides the time base for the Larmor frequency measurements, it is important that its deviations from the GPS clock are taken into account during the data processing.

Another parameter that changes with temperature is the power consumption. The input current goes up with falling temperatures, as shown in Figure 9-2. This means that the efficiency goes down at low temperatures. At the same occasion the power consumption for various input voltages has been measured. As can be seen in Figure 9-3 the dissipated power goes slightly up with rising voltages.

The present measurements do not allow to determine the temperature dependence of the returned NMR (Signal-Amplitude) from the sensor. The assessment of this parameter has to await a later test.
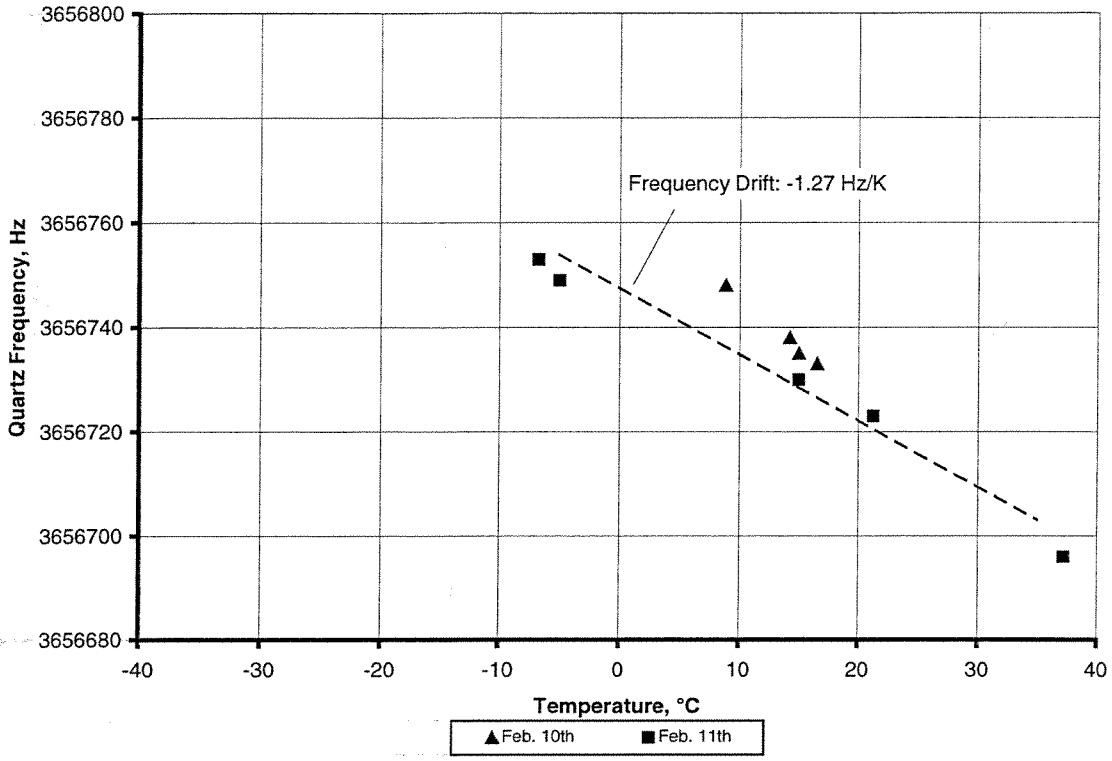
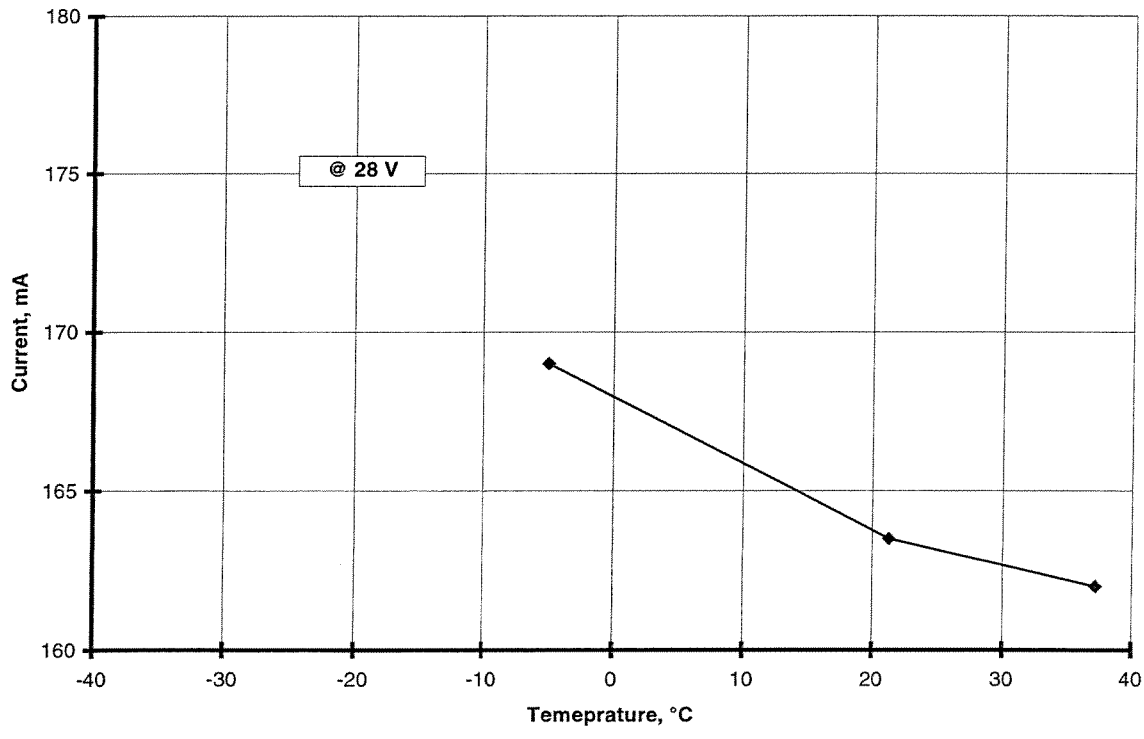Figure 9-1   Frequency dependence of the quartz oscillator on temperature

Figure 9-2   Current consumption of the OVM versus temperature
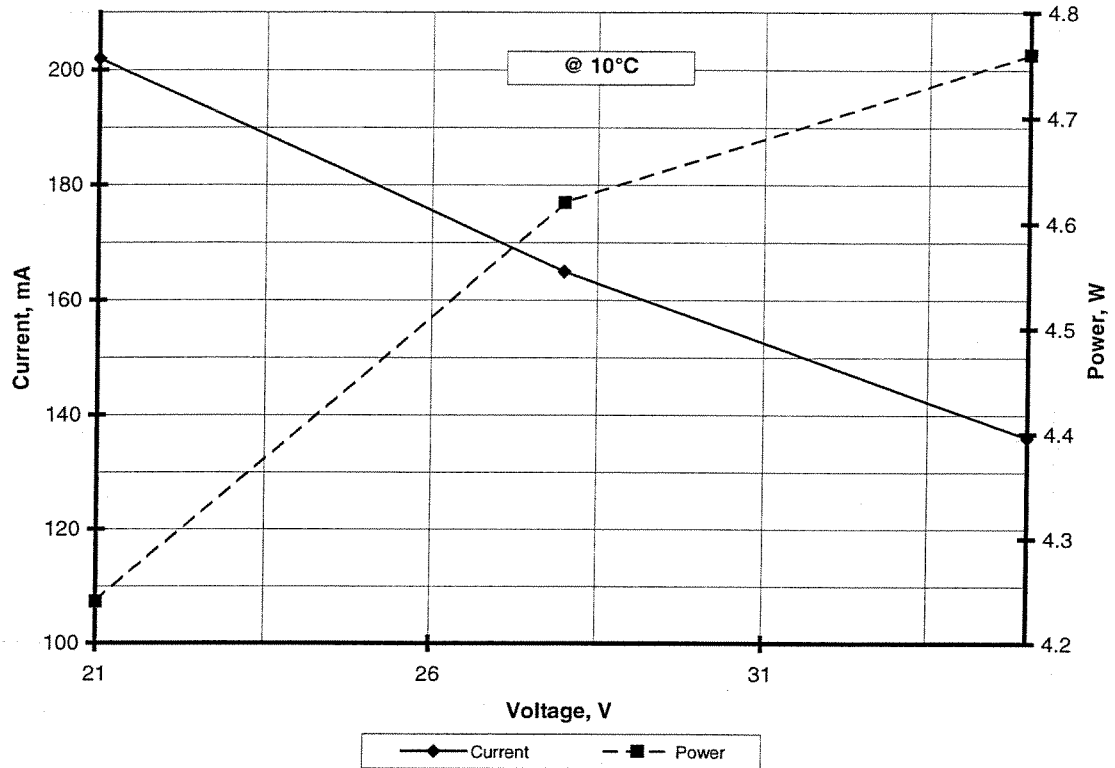
Figure 9-3   Power dissipation of the OVM versus input voltage

10 APPENDIX A

Residuals in nT between measured and calculated step response for the first 6 sec.
The step size in nT is given in the file name

File:	step10.dat	step20.dat	step50.dat	step100.dat
Time , s	Residuals , nT	Residuals , nT	Residuals , nT	Residuals , nT
	response: upward Start time : 22.65	response: upward Start time : 73.4	response: upward Start time : 128.8	response: upward Start time : 186.915
1	-7.205868E-02	1.218557E-02	-4.577637E-02	6.622314E-03
2	9.075403E-02	-4.829597E-02	2.687073E-02	-3.097534E-02
3	9.760809E-02	-0.0490756	5.074692E-02	-3.885651E-02
4	0.1091819	2.333307E-02	2.872086E-02	4.234314E-03
5	5.077267E-02	4.296398E-02	1.160431E-02	1.918793E-02
6	3.124952E-02	1.171875E-02	1.952744E-02	1.951599E-02
7	0	0	0	0
	response: downward Start time :52.5	response: downward Start time : 101.43	response: downward Start time : 160.53	response: downward Start time : 223.5
1	-9.113026E-02	6.144047E-02	-0.1853447	8.012772E-02
2	0.1866336	5.484581E-02	0.1808167	7.922745E-02
3	0.1516323	5.969429E-02	0.1556892	4.273987E-02
4	8.999729E-02	7.104874E-03	0.1218185	4.389572E-02
5	8.203793E-02	-3.091049E-02	5.081177E-02	2.347946E-02
6	-1.953077E-02	-1.951599E-02	4.296875E-02	4.296875E-02
7	0	0	0	0

File:	step200.dat	step500.dat	step1k.dat	step2k.dat
Time , s	Residuals , nT	Residuals , nT	Residuals, nT	Residuals , nT
	response: upward Start time : 3.475	response: upward Start time : 138.782	response: upward Start time : 7.64	response: upward Start time : 87.684
1	-0.1046829	8.889771E-02	0.4671631	1.534546
2	0.1031723	-0.2358093	-0.3058472	-1.036377
3	0.1407242	0.1109619	-3.234863E-03	-4.040527E-02
4	7.682037E-02	0.1472778	-2.514648E-02	-2.368164E-02
5	2.728271E-02	0.1155396	-4.016113E-02	-6.530762E-02
6	-0.0234375	3.015137E-02	1.165771E-02	-1.220703E-04
7	0	-6.103516E-05	0	0
	response: downward Start time : 61.645	response: downward Start time : 211.93	response: downward Start time : 48.56	response: downward Start time : 136.445
1	2.044678E-03	4.058838E-02	-0.9404297	-0.6695557
2	-3.442383E-02	-0.1435852	0.369751	0.7371216
3	-5.516052E-02	-9.051514E-02	9.307861E-02	0.1155396
4	-0.0222168	-7.006836E-02	0.0546875	6.280518E-02
5	1.976013E-02	-8.807373E-02	7.098389E-02	1.226807E-02
6	-3.904724E-02	-7.806396E-02	0.0703125	-0.046875
7	0	0	0	0

11 APPENDIX B

Residuals in nT between measured and calculated step response for the first 6 sec.
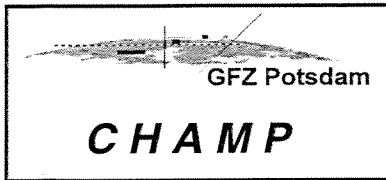The step size in nT is given in the file name

| File	step20.dat	step50.dat	step100.dat
	response: upward	response: upward	response: upward
Time , s	Residuals , nT	Residuals , nT	Residuals , nT
	Start time : 49.5	Start time : 241.501	Start time : 113.502
1	4.803848E-02	6.588745E-02	.1626053
2	-2.384186E-04	4.600525E-03	6.658936E-02
3	-1.577377E-03	-6.206131E-02	.1626663
4	-7.508278E-02	-.1320305	.1246643
5	-4.729843E-02	-7.923508E-02	.1305008
6	-5.861282E-02	-9.770584E-02	.1209869
	Start time : 81.5	Start time : 17.501	Start time : 145.502
1	.1379995	-.025383	.2358704
2	.2357597	-.2373581	.4373093
3	.2228069	-.141964	.5417175
4	.1122952	-.206131	.5150757
5	6.988144E-02	-.1925087	.2984619
6	8.982468E-02	-.1406746	.1014557
	Start time : 113.5	Start time : 49.501	Start time : 177.502
1	-7.473087E-02	-6.773376E-02	-7.810211E-02
2	-7.024956E-02	-5.554581E-02	-9.773254E-03
3	-3.338051E-02	-3.673935E-02	5.921936E-02
4	.0733242	-7.355118E-02	3.463745E-03
5	-1.995659E-02	-3.236389E-02	-7.262421E-02
6	-7.831573E-03	-7.036209E-02	3.895569E-02
	Start time : 145.5	Start time : 81.501	Start time : 209.502
1	-2.243996E-03	-2.561951E-02	-6.538391E-03
2	-.1396465	-.2875824	-.0821991
3	-.2232838	-.2155647	.0308609
4	-.20784	-.2412529	-8.31604E-03
5	-.148859	-.1612587	-1.403809E-02
6	1.169968E-02	-3.911209E-02	-1.182556E-02
	Start time : 177.5	Start time : 113.501	Start time : 241.502
1	.143218	6.904602E-04	.1107483
2	-9.487152E-03	-.2464294	-7.640076E-02
3	-7.475281E-02	-.1568184	.1044769
4	-6.721115E-02	-6.155777E-02	.1324997
5	-.1215153	-3.234863E-02	6.800079E-02
6	-5.080032E-02	1.166916E-02	.1209869
	Start time : 209.5	Start time : 145.501	Start time : 17.502
1	2.216339E-03	1.316071E-03	4.237366E-02
2	6.408119E-02	-4.338455E-02	-.218483
3	2.561188E-02	-3.162384E-03	-4.074097E-02
4	4.209709E-02	4.767227E-02	.0113678
5	1.129341E-02	7.701874E-02	-4.528046E-02
6	3.123093E-02	7.026291E-02	-8.213806E-02
	Start time : 241.5	Start time : 177.501	Start time : 49.502
1	-1.743698E-02	.1626511	-.1557312
2	-4.586029E-02	.3366585	-.5240936
3	-1.320457E-02	.3453255	-.419426
4	-7.898331E-02	.3287506	-.3167496
5	-.1801109	.1785698	-.1819992
6	-1.955032E-02	7.807541E-02	-7.041931E-02

12 APPENDIX C

Rotation about x axis

1032
1033
1105
1189
1293
1340
1318
1250
1175
1130
1090
1046
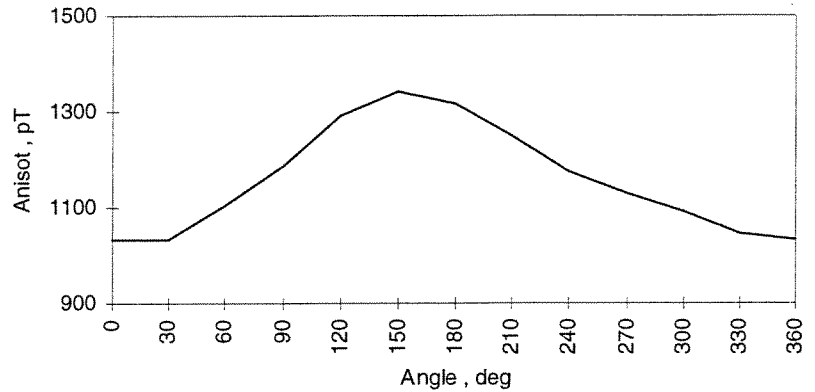
Rotation about y axis

835
1055
1200
1125
904
698
636
677
745
732
685
685
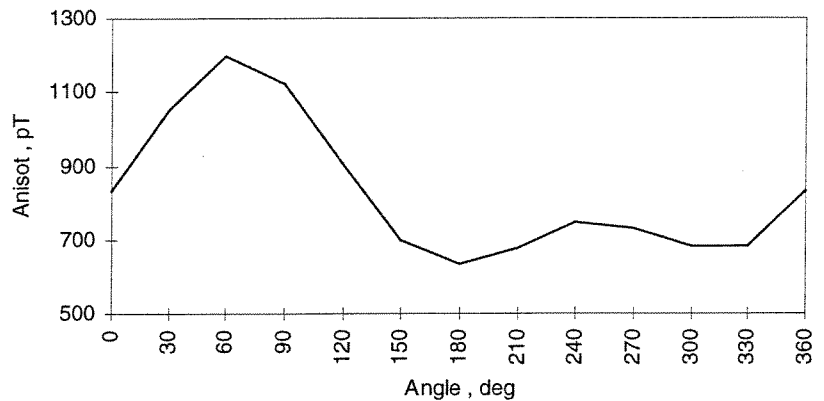
Heading error Xo, Yo, Zo in nT of the CHAMP OVM sensor
$\quad$ -.1781959 $\qquad$ -3.544685E-02 $\qquad$ -.1383213

Fourier Transform of Heading Error HEAD-E2

Rotation about x axis

n	a(n)	b(n)	A(n)	phi(n)
0.00	1166.75	0.00	1166.75	90.00
1.00	-144.17	35.45	148.47	-76.19
2.00	5.67	-29.73	30.27	169.21
3.00	-2.17	3.00	3.70	-35.84
4.00	0.50	0.00	0.50	89.97
5.00	3.34	-2.95	4.45	131.43
6.00	2.08	-0.00	2.08	90.00

Rotation about y axis

n	a(n)	b(n)	A(n)	phi(n)
0.00	831.42	0.00	831.42	90.00
1.00	105.52	195.37	222.04	28.37
2.00	-99.25	101.76	142.15	-44.29
3.00	-6.17	-0.33	6.18	-93.09
4.00	0.58	-1.01	1.17	150.00
5.00	0.15	0.80	0.81	10.62
6.00	2.75	-0.00	2.75	90.0